To be presented at the 7th Symposium held under the auspices of the US/USSR Technical Exchange Committee on Superconducting Power Transmission, Moscow, Sept. 1979.

MASTER

BNL-26712

CONF-790983--1

CALORIMETRIC MEASUREMENT OF AC LOSSES IN SUPERCONDUCTING CABLES OF SHORT LENGTHS*

J. E. Jensen
Brookhaven National Laboratory†
Associated Universities Inc.
Upton, NY 11973 USA

*Work supported by the U.S. Department of Energy.

†Operated by Associated Universities, Inc., Under Contract to the U.S. Department of Energy.

MASTER

ABSTRACT

The measurement of AC losses in superconducting cables by calorimetric means is necessary as a verification of electronic measurements on short high-current models and because the present method of electronic measurement is not applicable to longer cables with simultaneously applied high current and voltage. Consequently, after the first tests of Cable # 101 showed higher losses than anticipated using the electronic wattmeter measurements, it was decided to attempt to verify these measurements calorimetrically. This report presents the results of tests completed to date.

Introduction

During early current tests on BNL Cable # 101, there arose the question of verifying the electrical losses, as measured by the wattmeter, by calorimetric means. This type of measurement is also of interest for the large facility tests where the present wattmeter method is not applicable.

The first test was made in August 1978, with small success in measurement of the losses. The two old laboratory refrigerators, operating in parallel, were not sufficiently stable to maintain the system at temperature long enough to reach thermal equilibrium through the length of the line. Some temperature profiles were plotted which showed a change of slope, with and without current. However, it was also observed that the carbon resistor temperature sensors were not calibrated with sufficient accuracy and the measurement method introduced additional errors. It was apparent that $0.01^{o}K$ sensitivity would be necessary for the sensors and, assuming this was achieved, the calorimetric measurements appeared feasible.

Additional tests on Cable # 101 were performed during January and February 1979. The temperature instrumentation built into the cable remained the same but new germanium resistance sensors calibrated to 0.005°K between 4.2° and 30° K had been installed at both ends of the cable. In addition to these changes, a new CTI Model 1430 refrigerator had been received and installed. There were no problems in cooling the cable to any temperature desired, but there was still enough drifting of temperature to make it impossible to see the losses in a quantitative manner. It was also apparent that the existing carbon sensors in Cable # 101 would never be useful in these tests, but with all germanium sensors in a new cable it was felt that the losses could be measured to within a factor of 2 of the electrical measurements.

Cable # 102 Experimental Arrangement

During the preceding tests a new cable designated # 102 was being fabricated. This cable was instrumented with the precision-calibrated germanium temperature sensors. Figure 1 is a flow and instrumentation schematic of the test installation. High-pressure helium enters the west box, passing through the cable core and through the superconducting transformer, exiting at point 8. The electrical heater is used to raise the helium temperature at point 9 enough to ensure that liquid is not formed following expansion through the J-T valve or expansion engine. The test cable is enclosed by a 5 cm stainless steel tube which forms the high-pressure shell for the cable. The low-pressure helium, following expansion, passes from the east box to the west box through an annulus formed by the 5 cm tube containing the cable and the 10 cm tube which is the inner wall of the cryogenic enclosure. This low-pressure helium then returns to the refrigerator. In operation, the cable and its enclosures form the final heat exchanger of the refrigerator, with heat generated within the cable flowing to either the high- or low-pressure stream, depending upon which is lower in temperature. The heat influx through the enclosure insulation flows to the low-pressure stream. In this arrangement the cable, and its enclosure, becomes a counterflow heat exchanger with internal heat generation.

Temperature sensors 2 through 7 are located in the cable core in the high-pressure flow. Sensors 11 through 16 are in the annulus of the low-pressure return flow, and sensors 15 through 18 measure the temperature of the static high-pressure helium on the outside of the cable. The rest of the temperature sensors are located inside the high- and low-pressure piping. Pressure sensors and orifice-type flow meters are placed so that the mass flow and thermodynamic properties of the helium streams can be determined. The temperature sensors are connected to a mini-computer that measures the resistance and converts it to temperature in Kelvin which is then printed out as shown in Figure 2. The mini-computer also continuously samples temperature sensor 13 and raises or lowers the heater current to maintain this temperature constant at $7.25^{\circ} \pm 0.03^{\circ}$ K. This value and the sensor to be used were determined experimentally in order to maintain the temperature through the length of the cable as constant as possible without current on the cable.

Experimental Procedure

In order to establish a base line or static heat leak condition, the refrigeration rate was set by adjusting all of the refrigerator operating parameters with the trim heater controlled by the computer. The system was allowed to run for up to 24 hours without current on the cable, until temperature stability was reached. This was repeated a number of times during the two-week test. The same procedure was followed when current was applied to the cable, except that no changes were made on the refrigerator settings. Only the trim heater varied, and this was done by the computer to hold temperature 13 at the predetermined value. During tests with current on the cable, the system was allowed to operate until stability was reached. In one test the current was held at 500 rms A/cm for a period of 75 hours. Tests were made at 300, 400, 500 and 570 rms A/cm, with resulting data recorded for analysis.

Figure 2 shows the temperature data with no current on the cable (note heater power of 44.80 watts). Figure 3 is the same data plotted by the computer as a temperature profile for the test section. Figure 4 is the temperature data taken with 500 rms A/cm on the cable, and Figure 5 is the corresponding temperature profile plot. The heater power at this condition has been reduced to 35.97 watts in order to maintain the temperature at 13 within the pre-set limits.

Analysis of Data and Results

From the recorded temperature and pressure data, the enthalpies at all points and the densities, where required, were determined, using the computer functions developed by Arp.* The mass flow was calculated from the data for flow meters FM-1 and FM-2 and also from the relationship:

$$\dot{m} = \frac{Q_H}{h_9 - h_8}$$

where:

Q_H = trim heater power in watts

h_8 and H_9 are the enthalpies before and after the heater.

While making these calculations it was determined that the temperature at point 10, as recorded, was incorrect. Since all of the tests were run using the Joule-Thomson (J-T) valve, the enthalpy at 10 is required to be equal to the enthalpy at 9 because of isenthalpic expansion. Using the constant enthalpy relationship, a new temperature and density were calculated for each set of data and then these values were used in calculating the mass

*Arp, V., "New Forms of State Equations for Helium," Cryogenic 14, 593 (Nov. 1974).

flow at FM-1 and subsequent heat balances. The three mass flows calculated were within good experimental agreement and it was decided to use the value calculated by the heater balance because it fell between those of the two flow meters.

It is obvious that a great number of heat balances could be made from the data available, and quite a few were tried. The one presented here was selected because it gave the most consistent static loss results.

To find the electrically produced losses it is necessary to establish the static losses, which are then subtracted from the total losses found with current on the cable. The following relationships were used:

$Q_{HL} = \dot{m}\,(h_7 + h_{17} - h_1 - h_{10})$ heat leak, watts

$Q_T = \dot{m}\,(h_7 + h_{17} - h_1 - h_{10})$ total heat with current, watts

$Q_E = Q_T - Q_{HL}$ current-induced heat, watts

The heat leak, Q_{HL}, was calculated for a number of sets of data taken over a period of two weeks and the arithmetic average, 10.516 watts, used to calculate the electrical losses Q_E. Figure 6 shows the results of these calculations plotted against the current density. The upper curve was drawn using the calorimetric measurements, while the lower curve is from the electronic wattmeter. The slopes of the two curves are very nearly identical,with the calorimetric measurements a factor of 1.52 - 1.56 higher than the wattmeter measurements.

It would be very difficult to say that the wattmeter readings are in error from these data. The shorted end is included in both measurements. The losses in the transformer connection are not included in the wattmeter measurements, but it is possible that these losses are included in the calorimetric measurement, as well as some conduction losses through the connection because of heat generated in the transformer.

Conclusions

Progress has been made in instrumentation which makes it possible to measure the electrical losses in a superconducting power cable by calorimetric methods. The length of the test cable is a factor in such measurements because of the large losses which occur at each end. Longer test cables should help in this respect; however, longer cables with high current and voltage terminations will have larger end losses as well. Tests on larger systems will have to include very accurate temperature, pressure and flow instrumentation. The problem is further complicated by the difficulty in measuring the temperature of helium flowing in large, horizontal pipes or annuli because of the tendency towards stratification in low-velocity flow systems. It is possible to observe any increase in losses as the current is increased and this may be adequate monitoring for long cables. From a refrigeration point of view, it is all that is necessary since the refrigerator must remove all heat leaking into or produced by the cable in order for the cable to work properly.

Acknowledgement

This report represents the work of many people, the technicians who installed and ran the equipment as well as the engineers and physicists who designed the equipment and the tests. It is through the efforts of this excellent team that the achievements to date have been possible, and I am indebted to all of them.

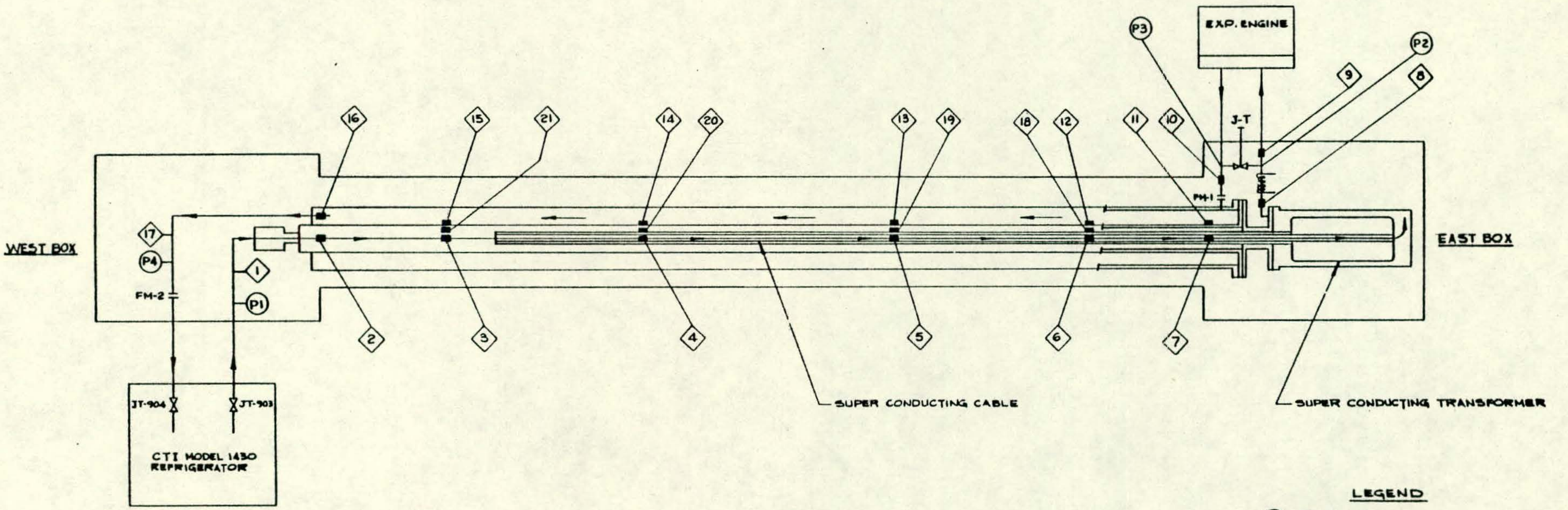

Fig. 1. Flow and Instrumentation Schematic.

16 Jun 79

Heater Power = 44.80 watts. 08:00:00

#	Ch	ID	Location	I (uA)	R (ohms)	T (kelvin)
1	15 LSC	#16 570	hi pres, He in from refrig	50.011	533.35	7.120
2	46 CryoCal	#6984	int core, 12.19 m (at W end)	50.088	457.04	7.191
3	45 CryoCal	#6412	int core, 10.97 m	50.096	464.97	7.194
4	44 CryoCal	#6283	int core, 7.75 m	50.086	479.81	7.187
5	43 CryoCal	#6942	int core, 4.52 m	50.086	462.77	7.201
6	42 CryoCal	#7272	int core, 1.30 m	50.082	401.64	7.202
7	41 CryoCal	#6973	int core, 0.15 m (east end)	50.079	464.58	7.204
8	33 LSC	#16 035	xmfr out, east end box	20.019	545.14	7.521
9	31 LSC	#16 588	xmfr, aft heater, b4 exp eng	20.019	262.60	9.798
10	32 LSC	#16 478	after expansion engine	20.019	420.99	7.565
11	21 LSC	#16 436	outside ss can, 0.15 m (east)	19.999	467.67	7.208
12	22 LSC	#16 216	outside ss can, 1.30 m	19.999	541.25	7.205
13	23 LSC	#16 280	outside ss can, 4.52 m	20.001	457.74	7.212
14	24 LSC	#16 193	outside ss can, 7.75 m	19.998	518.20	7.233
15	25 LSC	#16 287	outside ss can, 10.97 m	19.999	433.68	7.264
16	26 LSC	#16 285	outside ss can, 12.19 m	19.999	394.95	7.261
17	16 LSC	#16 571	low pres rtn to refrig	50.015	445.76	7.647
18	11 CryoCal	#6879	ext cable, 1.30 m from east	50.019	477.16	7.206
19	12 CryoCal	#6936	ext cable, 4.52 m from east	50.018	422.44	7.227
20	13 CryoCal	#6889	ext cable, 7.75 m from east	50.017	424.40	7.198
21	14 CryoCal	#6876	ext cable, 10.97 m from east	50.019	505.19	7.205

Figure 2. Steady State Temperatures, No Current in Cable.

Figure 3.

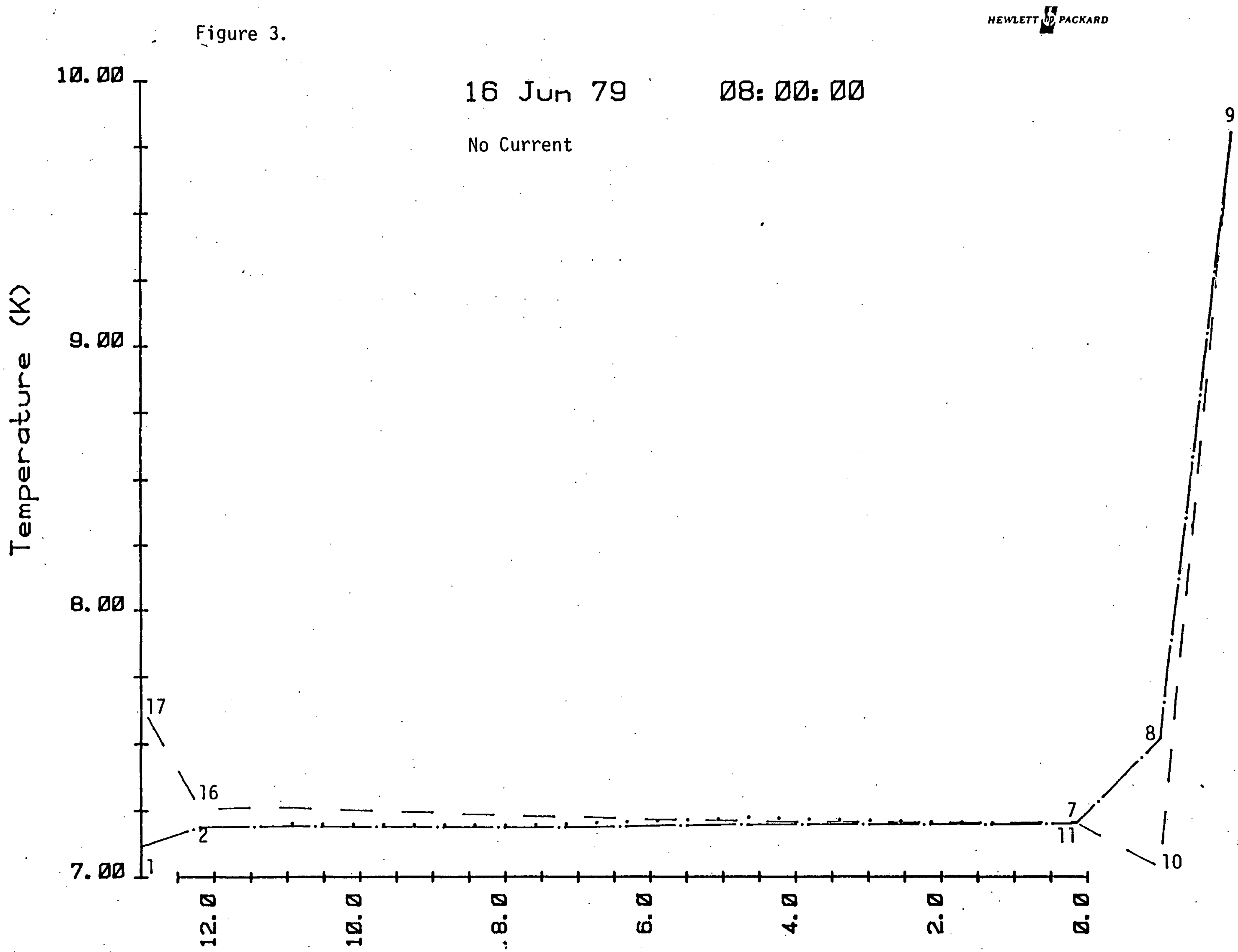

HEWLETT PACKARD
16 Jun 79
08:00:00
No Current
Temperature (K)
10.00
9.00
8.00
7.00
12.0
10.0
8.0
6.0
4.0
2.0
0.0
1
2
7
8
9
10
11
16
17

13 Jun 79

Heater Power = 35.97 watts. 09:00:00

#	Ch	ID	Location	I (uA)	R (ohms)	T (kelvin)
1	15	LSC #16 570	hi pres, He in from refrig	50.016	524.27	7.178
2	46	CryoCal #6984	int core, 12.19 m (at W end)	50.090	446.90	7.261
3	45	CryoCal #6412	int core, 10.97 m	50.098	450.40	7.294
4	44	CryoCal #6283	int core, 7.75 m	50.091	454.44	7.366
5	43	CryoCal #6942	int core, 4.52 m	50.089	429.75	7.431
6	42	CryoCal #7272	int core, 1.30 m	50.089	364.51	7.468
7	41	CryoCal #6973	int core, 0.15 m (east end)	50.090	425.60	7.487
8	33	LSC #16 035	xmfr out, east end box	20.022	459.49	8.181
9	31	LSC #16 588	xmfr, aft heater, b4 exp eng	20.023	255.84	9.908
10	32	LSC #16 478	after expansion engine	20.022	425.50	7.529
11	21	LSC #16 436	outside ss can, 0.15 m (east)	20.002	464.32	7.234
12	22	LSC #16 216	outside ss can, 1.30 m	20.001	533.00	7.260
13	23	LSC #16 280	outside ss can, 4.52 m	20.001	446.87	7.285
14	24	LSC #16 193	outside ss can, 7.75 m	20.002	507.54	7.310
15	25	LSC #16 287	outside ss can, 10.97 m	20.001	422.76	7.343
16	26	LSC #16 285	outside ss can, 12.19 m	20.001	385.73	7.333
17	16	LSC #16 571	low pres rtn to refrig	50.022	441.89	7.677
18	11	CryoCal #6879	ext cable, 1.30 m from east	50.022	462.38	7.303
19	12	CryoCal #6936	ext cable, 4.52 m from east	50.019	407.94	7.324
20	13	CryoCal #6889	ext cable, 7.75 m from east	50.019	407.99	7.307
21	14	CryoCal #6876	ext cable, 10.97 m from east	50.021	492.58	7.284

Figure 4. Temperatures With 500 rms A/cm on Cable.

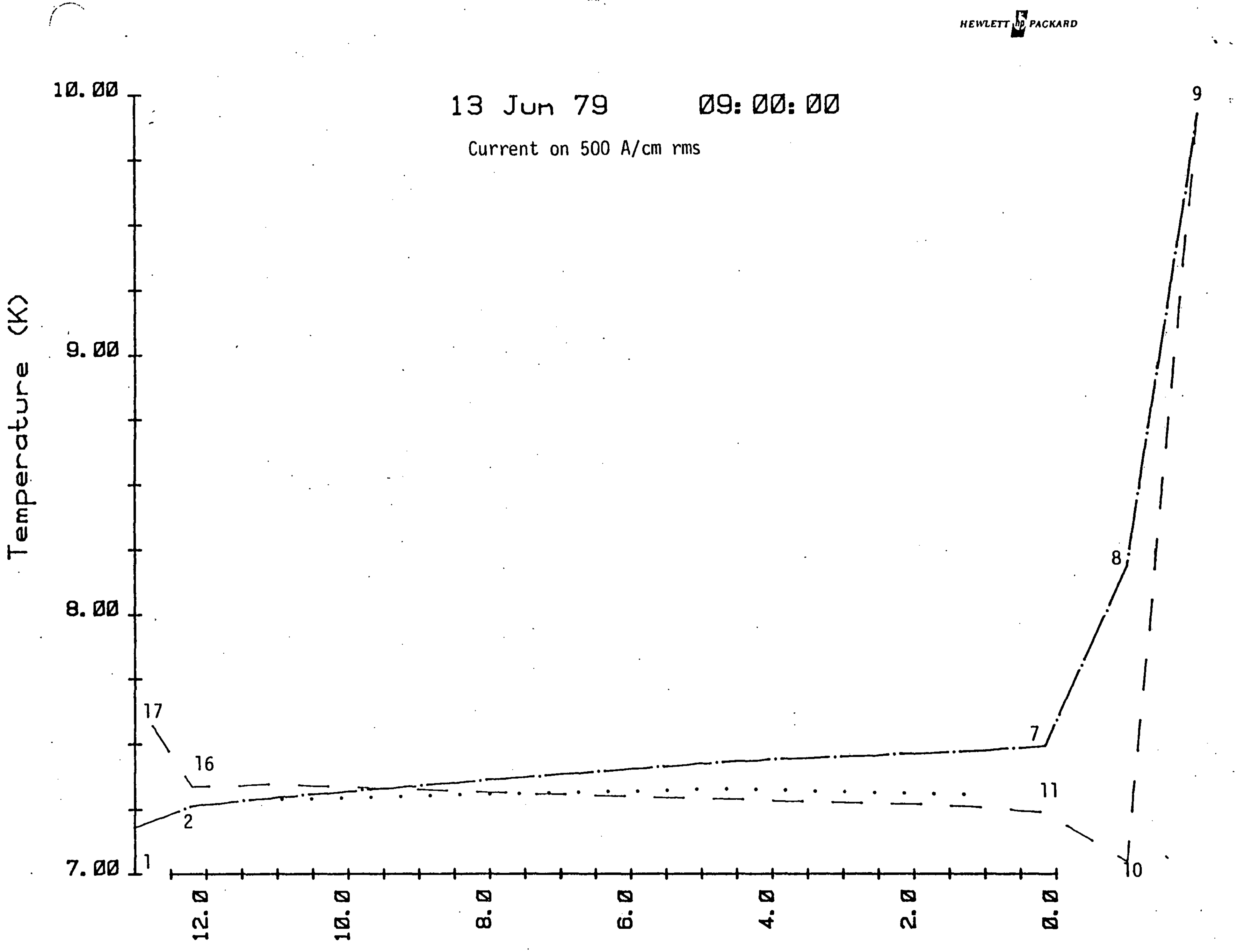
HEWLETT PACKARD
13 Jun 79 09:00:00
Current on 500 A/cm rms
Temperature (K)
10.00
9.00
8.00
7.00
1
2
7
8
9
10
11
16
17
12.0
10.0
8.0
6.0
4.0
2.0
0.0
Distance (m)
Figure 5

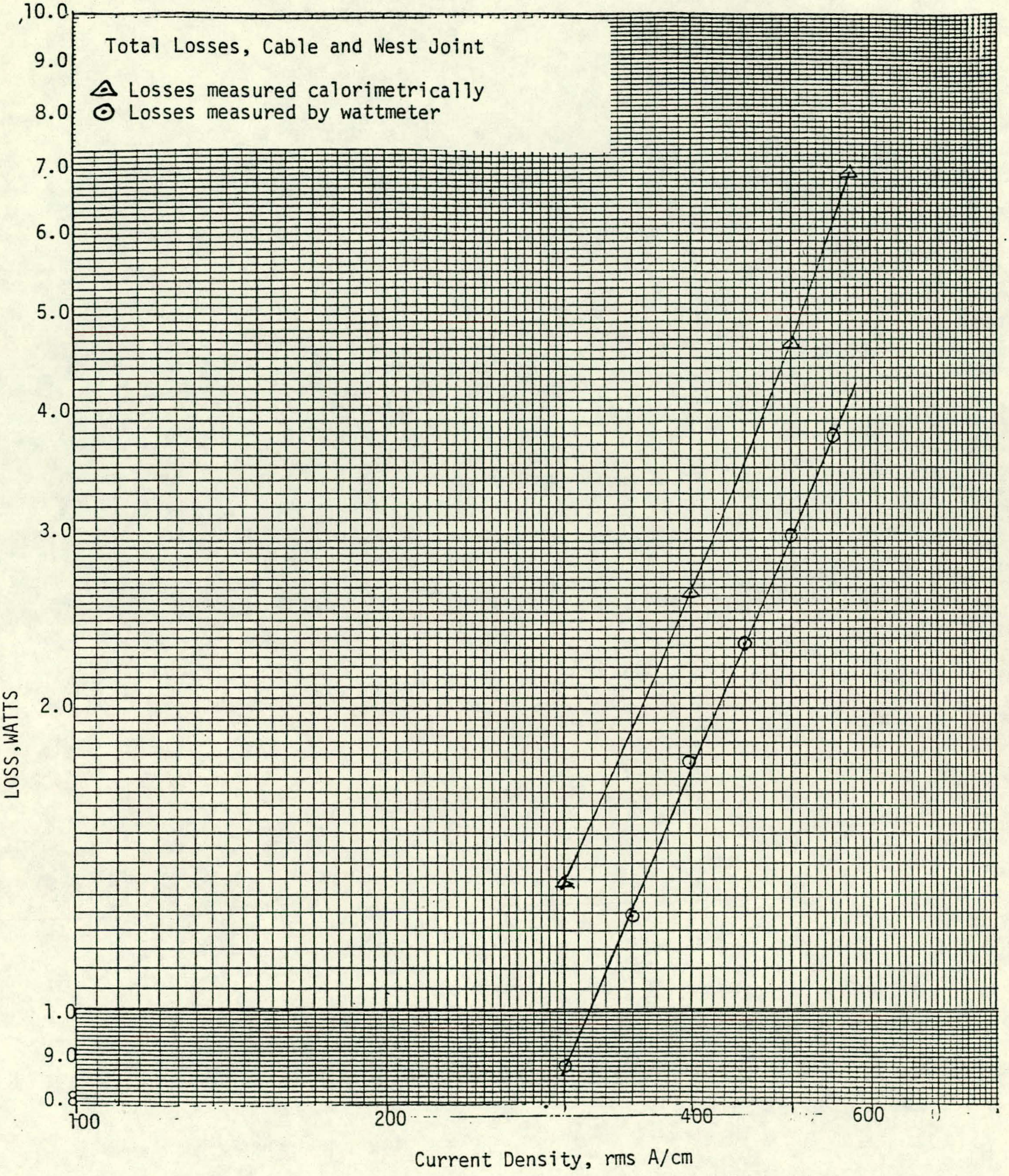

10.0
9.0
8.0
7.0
6.0
5.0
4.0
3.0
2.0
1.0
9.0
0.8
Total Losses, Cable and West Joint
Losses measured calorimetrically
Losses measured by wattmeter
LOSS,WATTS
100
200
400
600
Current Density, rms A/cm

Figure 6